

Tetrapalladium-Containing Polyoxotungstate [Pd^{II}₄(α -P₂W₁₅O₅₆)₂]¹⁶⁻: a Comparative Study

Natalya V. Izarova,^{†,||} Raisa I. Maksimovskaya,[‡] Sabine Willbold,[§] Paul Kögerler^{*,†,§}

[†] Peter Grünberg Institute – PGI 6, Forschungszentrum Jülich, D-52425 Jülich, Germany

[‡] Boreskov Institute of Catalysis, 630090 Novosibirsk, Russia

[§] Central Institute for Engineering, Electronics and Analytics – ZEA-3, Forschungszentrum Jülich, D-52425 Jülich, Germany

[§] Institute of Inorganic Chemistry, RWTH Aachen University, D-52074 Aachen, Germany

^{||} On leave from Nikolaev Institute of Inorganic Chemistry, 630090 Novosibirsk, Russia

KEYWORDS Palladium, Polyoxometalates, NMR spectroscopy.

ABSTRACT The novel tetrapalladium(II)-containing polyoxometalate [Pd^{II}₄(α -P₂W₁₅O₅₆)₂]¹⁶⁻ has been prepared in aqueous medium and characterized as its hydrated sodium salt Na₁₆[Pd₄(α -P₂W₁₅O₅₆)₂]·71H₂O by single-crystal XRD, elemental analysis, IR, Raman, multinuclear NMR and UV-Vis spectroscopy. The complex exists in *anti* and *syn* conformations which form in a 2 : 1 ratio and possesses unique structural characteristics in comparison with known {M₄(P₂W₁₅)₂} species. ³¹P and ¹⁸³W NMR spectroscopy are consistent with long-term stability of the both isomers in aqueous solutions.

INTRODUCTION

Pd^{II} complexes with polyoxotungstates (POTs) have attracted considerable attention during the last years as potential catalysts or precatalysts for various low-temperature transformations of organic substrates.^{1,2} On the other hand, the square-planar Pd^{II} coordination environment (in contrast to octahedral coordination characteristic for the first-row transition metals, the reactivity of which towards polyoxometalates (POMs) is widely investigated) opens possibilities to design polyanions with unique, so far not observed, structures and properties. In this context, a novel class of polyanions based exclusively on Pd^{II} and Au^{III} centers has been discovered in the past decade,^{2b,3} and very recently several unusual seleno- and tellurotungstates incorporating multinuclear Pd^{II} -based fragments reminiscent building blocks which constitute polyoxopalladate structures have been reported.⁴

Nevertheless the number of structurally characterized Pd-containing polyanions remains quite small in comparison with that of POMs incorporating 3d metals and lanthanides and the other examples include only a few Pd^{II} complexes with lacunary POTs⁵⁻⁹ as well as 1D polymers where Pd^{II} ions link paratungstate species into infinite chains.¹⁰ In this respect it was shown that monolacunary Lindqvist-, Keggin- and Wells-Dawson-type POTs form polyanions $[\text{Pd}^{\text{II}}_2(\text{W}_5\text{O}_{18})_2]^{8-}$, $[\text{Pd}^{\text{II}}_2(\alpha\text{-PW}_{11}\text{O}_{39})_2]^{10-}$ and *syn/anti*- $[\text{Pd}^{\text{II}}_2(\alpha_2\text{-P}_2\text{W}_{17}\text{O}_{61})_2]^{16-}$, respectively, where two Pd^{II} ions in a square-planar environment link together the two POM ligands.⁵ When the dilacunary derivatives of Keggin-type silicotungstate are reacted with Pd^{II} acetate, they form monomeric $[\gamma\text{-H}_2\text{SiW}_{10}\text{O}_{36}\text{Pd}_2(\text{CH}_3\text{COO})_2]^{4-}$ species there two Pd^{II} centers grafted on the vacant site of the POT are additionally bridged by two acetates.^{1m} Interaction of this complex with dicarboxylates led to carboxylate metathesis and formation of dimeric assemblies of the constitution $[\{(\gamma\text{-H}_2\text{SiW}_{10}\text{O}_{36}\text{Pd}_2)(\text{O}_2\text{C}(\text{CH}_2)_n\text{CO}_2)\}_2]^{8-}$ ($n = 1, 3, 5$).⁶ A number of sandwich-like

complexes with general formulae $[\text{Pd}_{3-y}(\text{WO}_2)_y(\text{XW}_9\text{O}_{34})_2]^{z-}$ ($E = \text{P}^{\text{V}}, \text{Si}^{\text{IV}}$)⁷ and $[\text{Pd}_{3-y}(\text{WO}_2)_y(\text{XW}_9\text{O}_{33})_2]^{z-}$ ($X = \text{As}^{\text{III}}, \text{Sb}^{\text{III}}, \text{Te}^{\text{IV}}$)⁸ are built by two trilacunary Keggin-type $\{\text{XW}_9\}$ units linked either via three Pd^{II} centers ($y = 0$) or via a belt comprising one Pd^{II} and two WO_2 groups ($y = 2$) or two Pd^{II} centers and one WO_2 group ($y = 1$), depending on the exact reaction conditions. Interaction of Pd^{II} with trilacunary bismuthotungstate $[\text{BiW}_9\text{O}_{33}]^{n-}$ resulted in the Krebs-type structure $[\text{Pd}_3(\text{H}_2\text{O})_9\text{Bi}_2\text{W}_{22}\text{O}_{76}]^{8-}$ where Pd^{II} ions are only weakly bound to the POT surface.⁹

At the same time almost no attention has been given to the reactivity of Pd^{II} towards lacunary derivatives of Wells-Dawson-type POMs, and the above-mentioned *syn* and *anti* isomers of $[\text{Pd}^{\text{II}}_2(\alpha_2\text{-P}_2\text{W}_{17}\text{O}_{61})_2]^{16-}$ are the only known structurally characterized Pd^{II} complexes with POTs of this structural type. Herein we report a novel sandwich-like polyanion $[\text{Pd}_4(\alpha\text{-P}_2\text{W}_{15}\text{O}_{56})_2]^{16-}$ (**1**) exhibiting unique structural features, which was obtained in the reactions of Pd^{II} ions with trilacunary Wells-Dawson type POT $[\alpha\text{-P}_2\text{W}_{15}\text{O}_{56}]^{12-}$ and isolated as the hydrated sodium salt $\text{Na}_{16}[\text{Pd}_4(\alpha\text{-P}_2\text{W}_{15}\text{O}_{56})_2] \cdot 71\text{H}_2\text{O}$ (**Na-1**) and the tetrabutylammonium salt $[(\text{C}_4\text{H}_9)_4\text{N}]_{15}[\text{HPd}_4(\alpha\text{-P}_2\text{W}_{15}\text{O}_{56})_2]$ (**TBA-1**).

RESULTS AND DISCUSSION

Synthesis. The polyanion **1** self-assembles in the reaction of Pd^{II} nitrate and $[\alpha\text{-P}_2\text{W}_{15}\text{O}_{56}]^{12-}$ in 0.5 M CH_3COONa medium in the pH range of 2 – 8 and the temperature range of 5 to 80 °C. Variation of the $\text{Pd}^{\text{II}} : \text{P}_2\text{W}_{15}$ ratio from 3 : 1 to 1 : 1 also does not influence the composition of the final product which is crystallized from the $\text{Pd}^{\text{II}} / \{\text{P}_2\text{W}_{15}\} / 0.5 \text{ M } \text{CH}_3\text{COONa}$ reaction systems, and **Na-1** has been isolated in all the cases as based on ³¹P NMR and IR spectroscopy as well as unit cell measurements. **Na-1** is well soluble in water (> 0.25 g / 1 ml) at room

temperature and is also soluble in 1 : 1 mixtures of H₂O/(CH₃)₂CO and H₂O/CH₃CN mixtures, and can be repeatedly recrystallized from water and 0.5 M CH₃COONa (pH 4.2).

The tetrabutylammonium salt, **TBA-1**, soluble in common organic solvents (*e.g.* CH₃CN, (CH₃)₂CO, CH₂Cl₂ *etc*), was prepared by dropwise addition of an aqueous solution of **Na-1** to an aqueous solution of TBAHSO₄, followed by washing of the obtained precipitate with plenty of water and its identity and purity was confirmed using IR, ³¹P NMR and C, H, N analysis.

Crystal structure analysis. Compound **Na-1** crystallizes in the triclinic symmetry in the space group *P*-1. The polyanions **1** possess a sandwich-like structure where two phosphotungstate units [α -P₂W₁₅O₅₆]¹²⁻ (= {P₂W₁₅}) are linked via a belt of four Pd^{II} centers (Fig. 1).

There is a complex disorder of [Pd₄(α -P₂W₁₅O₅₆)₂]¹⁶⁻ polyanions in the crystals of **Na-1** implying (1) a rotation of {P₂W₁₅} ligands by 60° which results in two symmetrically independent positions of {P₂W₁₅} with the relative occupancies of 66 and 34%, respectively; and (2) a rotation of the Pd₄ belt by +60° and -60° resulting in three symmetrically independent positions for the Pd₄ rhomb with the relative occupancies of 66% (non-rotated), 23% (rotated to +60°) and 11% (rotated to -60°). Such kind of disorder implies, on one hand, that part of the polyanions [Pd₄(α -P₂W₁₅O₅₆)₂]¹⁶⁻ can be turned relative to each other by either +60° or -60° during their packing in the crystals of **Na-1**. On the other hand, such hypothesis does not explain the non-equal distribution of the “rotated” and “non-rotated” positions for **1**, which is exactly reproducible from crystal to crystal. Another explanation is the turn of only one of the {P₂W₁₅} ligands in part of polyanions **1** relative to the remaining {Pd₄P₂W₁₅} unit by 60° which results in *syn/anti* isomerism with the *anti-1* to *syn-1* isomers ratio of 2 : 1, respectively (66% *vs* 34%). It should be noted that the rotation of {P₂W₁₅} *vs* {Pd₄P₂W₁₅} by either +60° or -60° would

equally lead to the *syn* derivative. The second scenario and the presence of both *anti* and *syn* isomers in this exact ratio have been confirmed by ^{31}P and ^{183}W NMR spectroscopy (*vide infra*).

The $\{\text{P}_2\text{W}_{15}\}$ ligands in **1** have typical Wells-Dawson structure with one W_3O_6 “capping” group missing and consist of two central tetrahedral PO_4 templates surrounded by 15 corner- and edge-shared WO_6 octahedra (Fig. 1). The polyanions possess C_{3v} symmetry with the C_3 axis passing through the two P^{V} ions. The 15 WO_6 octahedra can be formally divided into a W_3O_6 “cap” (gray in Fig.1) and an “inner” W_6O_{27} “belt” (dark-blue) assembled around one of the two $\text{P}^{\text{A}}\text{O}_4$ units (yellow tetrahedra), and an “outer” W_6O_{27} “belt” (light-blue) placed around the second $\text{P}^{\text{B}}\text{O}_4$ group (orange). Due to the missing second W_3O_6 “cap” the phosphotungstate $\{\text{P}_2\text{W}_{15}\}$ offers a so-called vacant or lacunary site with seven nucleophilic oxygen atoms suitable for coordination to various heterometals. Six of these oxygens coordinated to six W^{VI} centers of the “outer” W_6O_{27} “belt” form a nearly regular hexagon ($\text{O}\cdots\text{O}_{\text{average}}$: 3.08 Å) which is centered by an oxygen of the PO_4 group (Fig. S1, left). The W–O and P–O bond lengths in **1** are in the usual range.

All four Pd^{II} ions in the complex with $\{\text{P}_2\text{W}_{15}\}$ exhibit square-planar coordination. Two of them, situated on the opposite side of the Pd_4 rectangle, coordinate an oxygen atom of one of the WO_6 unit ($\text{Pd}-\text{O}$ 1.985(15) – 2.096(10) Å) and an oxygen atom of the $\text{P}^{\text{B}}\text{O}_4$ group ($\text{Pd}-\text{O}$ 2.029(15) – 2.057(18) Å). With respect to the geometry of the vacant site of $\{\text{P}_2\text{W}_{15}\}$ the two Pd^{II} ions of this structural type bind the two opposite oxygen atoms of the O_6 hexagon and the central O atom which they share between each other ($\text{Pd}\cdots\text{Pd}$ 3.121(4) Å). The type of coordination of these two Pd^{II} ions is the same for the both *anti* and *syn* isomers of **1**.

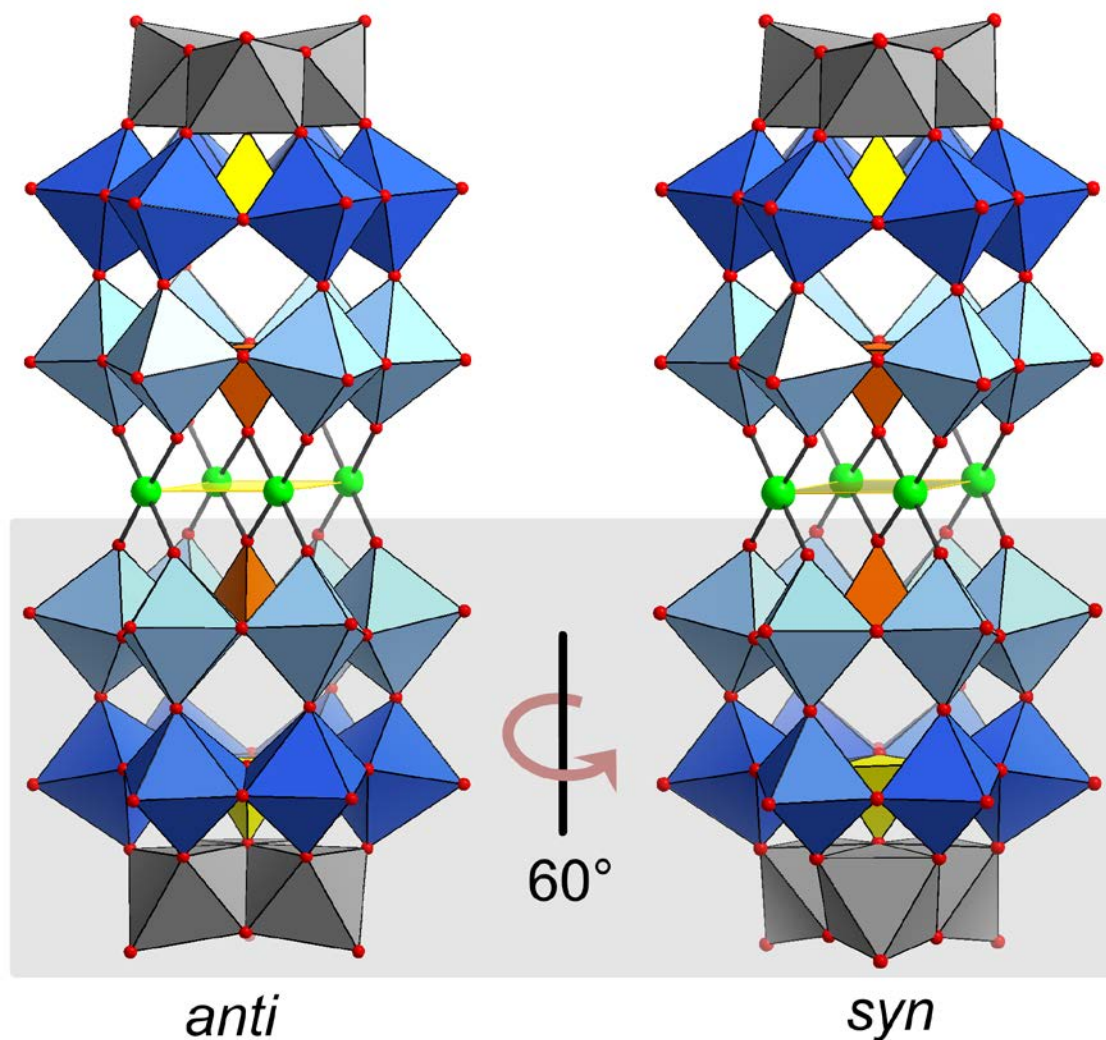


Figure 1. Structure of the *anti*-**1** (left) and *syn*-**1** (right) polyanions. WO_6 octahedra: W_3O_6 “cap”, gray; inner W_6O_{27} “belts”, blue; outer W_6O_{27} “belts”, light blue. $\text{P}^{\text{A}}\text{O}_4$ and $\text{P}^{\text{B}}\text{O}_4$: yellow and orange tetrahedra, respectively; Pd: green spheres, O: red. The Pd_4 plane is emphasized as a transparent yellow rhombus. Rotation of the lower $\{\text{P}_2\text{W}_{15}\}$ group by 60° transforms the isomers into each other.

Each of the other two Pd^{II} ions in the *anti* isomer of **1** coordinates two oxygens of the edge-shared W_2O_{10} unit of one POM ligand and two oxygens of the corner-shared W_2O_{11} unit of the second $\{\text{P}_2\text{W}_{15}\}$ species (Pd–O: 1.978(15) – 2.215(18) Å). Thus, the *anti*-**1** polyanions are centrosymmetric and belong to C_{2h} point symmetry group (Fig. 1, left). In terms of the geometry of the vacant site of the every $\{\text{P}_2\text{W}_{15}\}$ ligand these two Pd^{II} centers coordinate oxygens of two

opposite sides of a centered $\{O_6\}$ hexagon which remain non-coordinated by the Pd^{II} ions of the first structural type (Fig. S1, right). The $Pd \cdots Pd$ distance is $5.576(3) - 5.621(3)$ Å for the palladium centers of this structural type and $3.182(9) - 3.192(19)$ Å between the palladium(II) ions of the first and second structural types.

In the *syn* isomer the Pd^{II} centers of the second structural type are not equivalent: one of them binds oxygen atoms of edge-shared W_2O_{10} unit of the every $\{P_2W_{15}\}$ ligand and the second one, correspondingly, coordinates oxygens of the corner-shared W_2O_{11} groups of the each $\{P_2W_{15}\}$. Overall the *syn* derivative of **1** possesses idealized C_{2v} symmetry (Fig. 1, right).

The 2 : 1 ratio between the *anti* and *syn* isomers of **1** does not change by reacting Pd^{II} and $\{P_2W_{15}\}$ at various pH (from 2.0 to 7.8) or different temperatures (including reaction and crystallization of **Na-1** at 5 °C as well as prolonged heating of the reaction mixture at 80 °C). It also remains unchanged by performing the reaction in other Na^+ -containing media (*e.g.* 0.5 M Na_2SO_4 and $NaClO_4$ aqueous solutions) as based on ^{31}P NMR spectroscopy as well as the unit cell and, in some cases, complete crystal structure measurements. Importantly, ^{31}P NMR spectra of the reaction mixtures of Pd^{II} and $\{P_2W_{15}\}$ in CH_3COONa solutions showed that this ratio is not driven by crystal packing of the isomers in **Na-1** and appears already before crystallization (Fig. S6). It is also interesting to note that complex **1** does not form by reacting Pd^{II} and $\{P_2W_{15}\}$ in water based on ^{31}P NMR spectra of $Pd^{II} / \{P_2W_{15}\} / H_2O$ system.

The formation of the two isomers of $[Pd_4(\alpha-P_2W_{15}O_{56})_2]^{16-}$ is in agreement with the prior observation of *syn* and *anti* derivatives in Pd^{II} complexes with monolacunary Wells-Dawson phosphotungstates $\{\alpha_2-P_2W_{17}\}$.^{5c} However in that case the significantly different shape of the *anti* and *syn* isomers of $[Pd_2(\alpha_2-P_2W_{17}O_{61})_2]^{16-}$ resulted in the different solubility of their alkali metal salts and thus allowed isolations of the both derivatives in the pure state. Unfortunately the

relatively high C_{3v} symmetry of $\{P_2W_{15}\}$ ligands and the very similar stereochemistry of *anti*-**1** and *syn*-**1** render their separation hardly feasible at the moment. However we are trying to isolate other (Rb^+ , Cs^+ or organic) salts of **1** with the aim of separating the isomers or to changing their relative ratio.

It is also interesting to compare the structure of **1** with that of well-known $[M_4(H_2O)_2(P_2W_{15}O_{56})_2]^{n-}$ ($= \{M_4(P_2W_{15})_2\}$) complexes formed by octahedrally-coordinated transition metal centers ($M = Mn^{II}$, Fe^{III} , Co^{II} , Ni^{II} , Cu^{II} , Zn^{II} , and Cd^{II}).¹¹ Like in **1** the typical structure of a $\{M_4(P_2W_{15})_2\}$ complex comprises a tetrametal belt $M_4(H_2O)_2$ sandwiched between two $\{P_2W_{15}\}$ phosphotungstates. At the same time the higher coordination number six of the M^{m+} centers in $M_4(H_2O)_2$ (comparing with $CN = 4$ for Pd^{II} in **1**) leads to significant structural differences. Thus every O atom associated with the $P^B O_4$ group at the lacunary site of $\{P_2W_{15}\}$ in $\{M_4(P_2W_{15})_2\}$ is coordinated not by two as in **1** but by three M^{m+} ions at the same time. Two of the four M^{m+} centers in $M_4(H_2O)_2$ coordinate to $P^B O_4$ groups of both $\{P_2W_{15}\}$ ligands (which could be compared with the two Pd^{II} of the first structural type in **1**), whereas the remaining two M^{m+} ions only bind to a $P^B O_4$ of only one $\{P_2W_{15}\}$ ligand. This results in a parallel shift of the main axes of the $\{P_2W_{15}\}$ units in $\{M_4(P_2W_{15})_2\}$ while the C_3 axes of each $\{P_2W_{15}\}$ unit coincide and pass through the center of the Pd_4 rhombus (Fig. S2). From an alternative point of view, the three MO_6 octahedra in the $M_4(H_2O)_2$ belt coordinating to $P^B O_4$ form $\{M_3P_2W_{15}\}$ units akin to β -type Wells-Dawson structures, and the common $\{M_4(P_2W_{15})_2\}$ structure can be regarded as a centrosymmetrical $\beta\beta$ -isomer.¹¹ In the case of $M = Co^{II}$ it was shown that a mixture of $\beta\beta$ - and $\alpha\beta$ - isomers (which differ from $\beta\beta$ by a 60° rotation of one of the $\{P_2W_{15}\}$ units with respect to the $\{M_4P_2W_{15}\}$ part) co-exist in reaction mixtures at neutral pH values.¹¹ⁱ This is in direct analogy with *anti/syn* isomerism in the $\{Pd_4(P_2W_{15})_2\}$ complex.

In summary, the Pd^{II}-based complex **1**, {Pd₄(P₂W₁₅)₂}, in comparison to conventional {M₄(P₂W₁₅)₂}-type structures exhibits structural similarities, in particular the similar rhombic arrangement of the four metal centers of the inner belt of the polyanions and the ability to form isomers which differ by 60° rotation of one of the {P₂W₁₅} groups with respect to the {M₄P₂W₁₅} unit. At the same time, **1** displays unique structural characteristics imparted by the square-planar coordination environment of Pd^{II} ions, implying the local C₃ axes of the two {P₂W₁₅} groups coincide and formation of the *syn* isomers also in acidic media.

The structure of **1** is also unique in comparison with structurally characterized sandwich-like Pd^{II} complexes of the trilacunary Keggin-type species [A- α -(XO₄)W₉O₃₀]ⁿ⁻ and [B- α -(XO₃)W₉O₃₀]ⁿ⁻ (= {XW₉}), {Pd₃(XW₉)₂}.⁷⁻⁸ Compared to {XW₉} the vacant site of {P₂W₁₅} offers an additional central oxygen atom of the P^BO₄ group due to the different orientation of the XO₄ tetrahedron in the B- α - and A- α -trilacunary POT derivatives (Fig. S3). Also in {B- α -XW₉} this additional oxygen is absent and replaced by a lone pair on the central X^{III/IV} heteroion (X = As^{III}, Sb^{III}, Te^{IV}). This feature allows for coordination of four Pd^{II} centers in **1** while the sandwich-like complexes of Pd^{II} with {XW₉} POTs contain only up to three noble metal ions. On the other hand, Ratiu and co-workers in 1998 proposed formation of [Pd₄(B- α -PW₉O₃₄)₂]¹⁰⁻ polyanions based on UV-Vis, photocolourimetry and conductometry data.¹¹ {Pd₄(B- α -PW₉)₂} should possess a structure similar to **1** where the {P₂W₁₅} ligands are replaced by [B- α -PW₉O₃₄]⁹⁻ POTs. However there still is no structural evidence for the formation of a complex with {Pd₄(B- α -PW₉)₂} stoichiometry and our attempts to isolate such derivative so far failed, leading to the well-characterized^{7a-c} [Pd₃(A- α -PW₉O₃₄)₂]¹²⁻ species.

The IR spectrum of Na-**1** exhibits three absorption bands at 1090, 1065 and 1016 cm⁻¹ which could be assigned to vibrations of P–O bonds. They could be compared with the P–O vibrations

bands at 1130, 1086 and 1009 cm^{-1} for $\text{Na}_{12}[\alpha\text{-P}_2\text{W}_{15}\text{O}_{56}]\cdot 24\text{H}_2\text{O}$ ($\text{Na}\text{-}\{\text{P}_2\text{W}_{15}\}$) (Fig. S4 and refs. 11a, 12) and at 1090 and 1012 cm^{-1} for $\text{K}_6[\alpha\text{-P}_2\text{W}_{18}\text{O}_{62}]\cdot 14\text{H}_2\text{O}$ (Fig. S4 and refs. 12, 13). The disappearance of the band at 1130 cm^{-1} characteristic for non-coordinated $\{\text{P}_2\text{W}_{15}\}$ and appearance a new band at 1065 cm^{-1} is in agreement with the coordination of one of the oxygen atoms of PO_4 group at the lacunary site of the $\{\text{P}_2\text{W}_{15}\}$ ligands by Pd^{II} in **1**. The band characteristic for terminal $\text{W}=\text{O}$ bonds appears at 941 cm^{-1} . The set of bands in the range of 909 to 767 cm^{-1} could be assigned to vibrations of $\text{W}-\text{O}-\text{W}$ and $\text{W}-\text{O}-\text{Pd}$ bonds. The significant shift of these bands comparing to the $\text{W}-\text{O}-\text{W}$ bands in non-coordinated $\{\text{P}_2\text{W}_{15}\}$ (see Fig. S4) is also consistent with formation of a coordination complex between Pd^{II} and $\text{Na}\text{-}\{\text{P}_2\text{W}_{15}\}$ in **Na-1**. A band at 563 cm^{-1} which is absent in the spectrum of $\text{Na}\text{-}\{\text{P}_2\text{W}_{15}\}$ corresponds to $\text{Pd}-\text{O}$ valence bands.¹⁴ The IR spectrum of **TBA-1** exhibits similar features and additional bands corresponding to $\text{C}-\text{C}$, $\text{C}=\text{C}$ and $\text{C}-\text{H}$ vibrations of the TBA^+ counteranions (Fig. S5).

NMR spectroscopy. The room temperature ^{31}P NMR spectrum of **1** (Fig. 2) exhibits three signals at -3.4 , -3.6 and -14.6 ppm with the relative intensities of 2 : 1 : 3 which could be compared with the signals at $+0.1$ and -13.3 ppm for the non-coordinated $\{\text{P}_2\text{W}_{15}\}$ ligands¹² and the lines at -4.3 and -14.3 ppm for $\{\text{Zn}_4(\text{P}_2\text{W}_{15})_2\}$.^{11b} The most intense signal at -14.6 ppm stems from the $\text{P}^{\text{A}}\text{O}_4$ group of the $\{\text{P}_2\text{W}_{15}\}$ ligands and it appears to be not sensitive to the *anti*-/*syn*-isomerization. The two downfield signals originate to the $\text{P}^{\text{B}}\text{O}_4$ close to the Pd_4 belt. Based on relative intensities of these two signals which are in a very good agreement with the solid-state X-ray data the signal at -3.4 ppm could be assigned to the *anti-1* isomer while the signal at -3.6 ppm belongs to the *syn-1* derivative. Spectra measured at 278 K (Fig. S7) and 353 K (Fig. S8) both exhibit the same three signals, although their chemical shifts differ slightly compared to the room temperature spectrum (-2.9 , -3.1 and -14.1 ppm at 278 K and -4.0 , -4.2 and -15.2

ppm at 353 K). The relative intensity of the two downfield signals in these spectra indicates the same 2 : 1 ratio between the *anti* and *syn* isomers of **1** confirming the absence of dynamic phenomena associated with the complex dissociation and isomerization in aqueous medium at various temperatures.

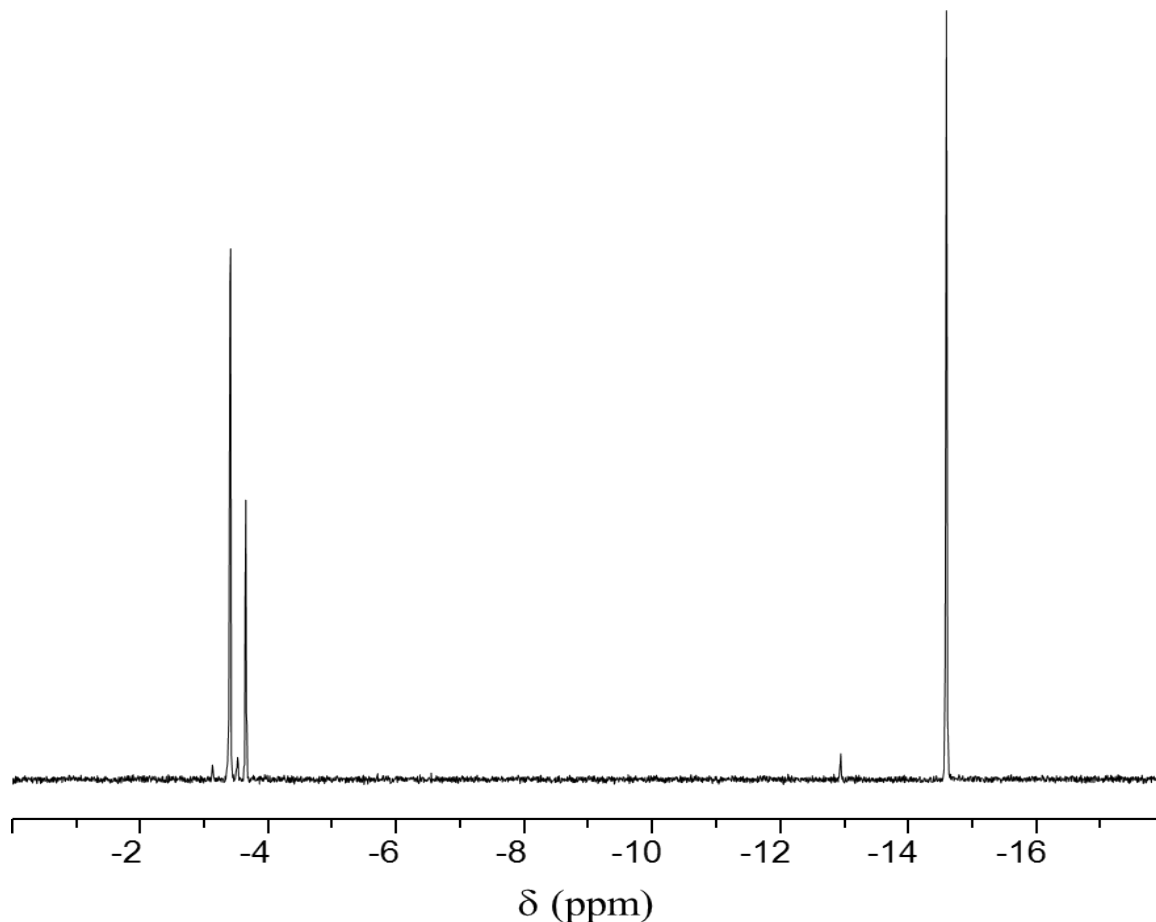


Figure 2. Room temperature ^{31}P NMR spectrum of **Na-1** redissolved in H_2O / D_2O (the three small signals belong to minor impurities which do not exceed 2%).

The spectrum remains unchanged for a long period of time, indicating high solution stability of the polyanions **1** in aqueous medium.

The room temperature ^{183}W NMR spectrum of aqueous **Na-1** solution exhibits 15 signals (Fig. 3) in a good agreement with the expected pattern, based on the solid-state structure. The $\{\text{P}_2\text{W}_{15}\}$

ligands in both *anti* and *syn* isomers of **1** acquire local C_s symmetry with the vertical mirror plane intersecting the two Pd^{II} ions of the second structural type and one of the W^{VI} center of the W_3O_{13} “cap”. The mirror plane divides the W centers of each $\{\text{P}_2\text{W}_{15}\}$ unit into seven pairs of symmetry-equivalent atoms and the unique polar W site, similar to the patterns observed for the $\{\text{M}_4(\text{P}_2\text{W}_{15})_2\}$ series ($\text{M} = \text{Co}, \text{Cu}, \text{Zn}$).^{11b} Accordingly, the observed 15-line spectrum can be attributed to the 2 : 1 mixture of the C_{2h} -symmetric *anti* and the C_{2v} -symmetric *syn* isomers of **1**, each of which giving 8 signals in a 2 : 2 : 2 : 1 : 2 : 2 : 2 : 2 intensity ratio. Thus the more intense signals at -87 (relative intensity 4, $J_{\text{W-O-P}}$ 1.4 Hz), -155 (4, $J_{\text{W-O-P}}$ 0.8 Hz), -158 (2, $J_{\text{W-O-P}}$ 1.5 Hz), -159.5 (4, $J_{\text{W-O-P}}$ 1.8 Hz), -236 (4, $J_{\text{W-O-P}}$ 1.9 Hz), -243 (4, $J_{\text{W-O-P}}$ 1.75 Hz), -245.4 (4, $J_{\text{W-O-P}}$ 1.65 Hz) belong to the *anti*-isomer of **1** while the weaker signals at -91 (2), -156 (2), -159 (1), -160.4 (2), -236.6 (2), -243.6 (2) and -244.6 (2) could be assigned to the *syn* derivative. The peak at -136 (6) is attributed to the overlapping signals from both *anti*-**1** and *syn*-**1** species.

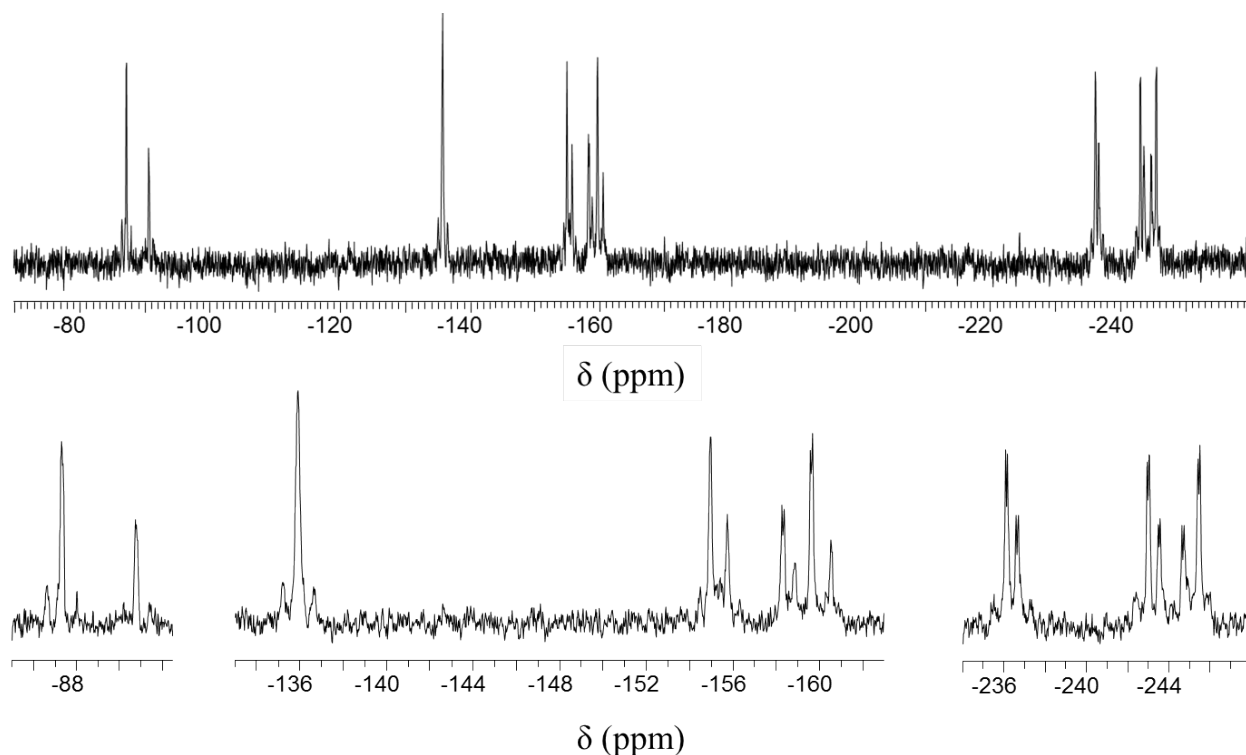


Figure 3. Room temperature ^{183}W NMR spectrum of **Na-1** redissolved in H_2O / D_2O after exponential multiplication with a line broadening of 0.5 Hz (top); zoom into the signals (bottom)

Based on their lower relative intensity, the signals at -158 ppm (*anti-1*) and -159 ppm (*syn-1*) are attributed to the unique polar W^{VI} centers of the $\{\text{P}_2\text{W}_{15}\}$ ligands. The chemical shift values for these signals are in a good agreement with the literature data for $[\alpha\text{-H}_x\text{P}_2\text{W}_{15}\text{Nb}_3\text{O}_{62}]^{(9-x)-}$,¹⁵ $[\alpha\text{-H}_3\text{P}_2\text{W}_{15}\text{O}_{59}\{\text{Al}(\text{OH}_2)\}_3]^{6-}$ ¹⁶ and $[\alpha\text{-P}_2\text{W}_{15}\text{Ti}_3\text{O}_{62}]^{12-}$ ¹⁷ polyanions with C_{3v} symmetry for which the signals corresponding to the W^{VI} centers of the W_3O_6 “caps” appear at -148.0 , -156.6 and -148.3 ppm, respectively, as well as with observation of signal at -150.4 ppm for the unique W^{VI} centers in $\{\text{Zn}_4(\text{P}_2\text{W}_{15})_2\}$.^{11b} Unfortunately very close spacing of the signals for the both isomers complicates their direct assignment based on $J_{\text{W-O-W}}$ values, however the attribution of the remaining signals can be based on the similarity to the ^{183}W NMR spectrum of the related $\{\text{Zn}_4(\text{P}_2\text{W}_{15})_2\}$ ^{11b} complex (for which 2D INADEQUATE $^{183}\text{W}\{^{31}\text{P}\}$ NMR measurements allowed unambiguous attribution of all peaks) and logical reasoning. Thus the three closely spaced upfield signals (at -236 , -243 and -245.4 for *anti-1* and -236.6 , -243.6 and -244.6) most likely belong to the W^{VI} centers of the inner W_6O_{27} “belt” of $\{\text{P}_2\text{W}_{15}\}$ (arranged around the $\text{P}^{\text{A}}\text{O}_4$ group like the W_3O_6 “cap”). This proposition is in a good agreement with observation of the signals for the inner W_6O_{27} “belt” of $\{\text{P}_2\text{W}_{15}\}$ units in $\{\text{Zn}_4(\text{P}_2\text{W}_{15})_2\}$ at -238.4 , -243.4 , -244.7 ppm. The signal at -159.5 ppm shows the same splitting due to $J_{\text{P-O-W}}$ coupling (~ 1.8 Hz) as that of the unique polar W^{VI} center. This suggests that the signals at -159.5 ppm (for *anti-1*) and -160.4 ppm (for *syn-1*) also belong to the W centers of the W_3O_{13} “caps” connected with the P^{B} atom through the O atom that is common to all the three tungstens. Then the remaining three signals that are shifted to significantly higher frequencies relative the spectrum range of $\{\text{Zn}_4(\text{P}_2\text{W}_{15})_2\}$ relate to the W atoms connected to palladium. It is also logical to suggest that the

six W^{VI} centers close to the lacunary site of the $\{P_2W_{15}\}$ units in **1** are less shielded compared to the other W^{VI} centers due to the square-planar coordination environment of the Pd^{II} ions and subsequently give the three most downfield signals (at -87 , -136 and -155 ppm for *anti*-**1** and -91 , -136 and -156 ppm for *syn*-**1**). At that the downfield shift of these signals in comparison with the corresponding signals in the ^{183}W NMR spectrum for $\{Zn_4(P_2W_{15})_2\}^{11b}$ is consistent with a weaker binding of the $\{P_2W_{15}\}$ ligands to the Pd^{II} centers in **1** than to the Zn^{II} centers in $\{Zn_4(P_2W_{15})_2\}$, which is in full agreement with the different coordination geometries of the Pd^{II} and Zn^{II} centers in these structures. We further hypothesize that the signal at -136 ppm may possibly correspond to the W^{VI} centers binding the oxygens coordinated by Pd^{II} centers of the first structural type as such W^{VI} centers have very similar coordination environment in the both *anti*-**1** and *syn*-**1** derivatives.

UV-Vis spectroscopy. The solutions of **Na-1** were further examined using absorption spectroscopy. The UV-Vis spectrum of **Na-1** in 0.5 M CH_3COONa aqueous solution (pH = 4.3), shown on the Fig. S7, exhibits strong absorption maximum at 236 nm ($\epsilon = 166167\text{ M}^{-1}\text{cm}^{-1}$) followed by a broad shoulder at about 292 nm ($\epsilon = 81495\text{ M}^{-1}\text{cm}^{-1}$) in the UV light area and a less intense absorption maximum at 477 nm ($\epsilon = 2374\text{ M}^{-1}\text{cm}^{-1}$) in the visible light area. The spectrum remains unchanged for at least 1 week for both more (6.7×10^{-4} M) and less (4.7×10^{-5} M) concentrated solutions confirming the stability of polyanions **1** in 0.5 M CH_3COONa aqueous medium at pH 4.3.

The spectra of **Na-1** solutions in 1 M CH_3COOH (pH 2.0) and 1 M CH_3COONa at various pH are shown on the Fig. S10. The solutions were prepared independently taking equal amounts of **Na-1** and equal amounts of the corresponding solvent. The obtained spectra showed highest absorption at about 477 nm in the solutions with a pH range of 2 to 4 suggesting the highest

stability of **1** in these media. The spectra at pH 2.0 and 4.0 remained unchanged for at least 1 day while it was not possible to monitor the stability of **1** in the solutions with higher pH values due to lower solubility and recrystallization of **Na-1** which occurs within several hours.

CONCLUSIONS

In our investigation of the reactivity of Pd^{II} ions towards trilacunary derivative of Wells-Dawson-type phosphotungstates [α -P₂W₁₅O₅₆]¹²⁻ in 0.5 M CH₃COONa media, the tetranuclear sandwich-like complex [Pd₄(α -P₂W₁₅O₅₆)₂]¹⁶⁻ was found to self-assemble in a wide range of pH, Pd^{II} : {P₂W₁₅} ratios and reaction temperatures. The [Pd₄(α -P₂W₁₅O₅₆)₂]¹⁶⁻ clusters exist as *syn* and *anti* isomers which vary in the relative orientation of the two {P₂W₁₅} ligands and form in a 2 : 1 ratio. Due to square-planar Pd^{II} coordination the title structure differs from conventional (transition metal-substituted) {M₄(P₂W₁₅)₂} species despite the similar rhombic arrangement of the four heterometal ions in these complexes. The arrangement of Pd^{II} centers in **1** also differs markedly from Pd^{II} complexes with trilacunary Keggin-type polyoxotungstates because of the slightly different structure of the vacant sites in these POTs. ³¹P and ¹⁸³W NMR spectroscopy demonstrated a long-term solution stability of polyanions **1** in aqueous media.

EXPERIMENTAL SECTION

General methods and materials. The reagents were used as purchased without further purification. Na₁₂[α -P₂W₁₅O₅₆] \cdot 24H₂O was obtained according to the reported procedure^{11a,12} starting from K₆[α -P₂W₁₈O₆₂] \cdot 14H₂O.^{12,13} Elemental analysis results (ICP-OES) were obtained from Central Institute for Engineering, Electronics and Analytics (ZEA-3), Forschungszentrum Jülich GmbH (D-52425 Jülich, Germany). Vibrational spectra were recorded on a Bruker VERTEX 70 FT-IR spectrometer coupled with a RAM II FT-Raman module (1064 nm Nd:YAG laser) on KBr disks for the FT-IR and the solid material for the Raman measurements. UV-Vis

spectra were measured using 10 mm quartz cuvettes on Analytik Jena Specord S600 spectrophotometer. ^{31}P NMR spectra were recorded at room temperature in 5 mm tubes using a Bruker Avance 600-MHz spectrometer equipped with a prodigy probe, operating at 242.95 MHz for ^{31}P and with a Varian Inova 400 MHz spectrometer equipped with an Auto-X-PFG-probe and with resonance frequency of 161.834 MHz. Chemical shifts are reported with respect to 85% H_3PO_4 ; all chemical shifts downfield of the reference are reported as positive values. ^{183}W NMR spectra of **Na-1** solution in H_2O / D_2O ($c \sim 1 \times 10^{-2}$ M) were recorded in 10 mm tubes on a Bruker Avance 400 MHz instrument at room temperature with a resonance frequency of 16.67 MHz. The chemical shifts are reported with respect to 1 M Na_2WO_4 aqueous solution as a reference.

Synthesis of $\text{Na}_{16}[\text{Pd}_4(\alpha\text{-P}_2\text{W}_{15}\text{O}_{56})_2] \cdot 71\text{H}_2\text{O}$ (Na-1). A sample of $\text{Na}_{12}[\alpha\text{-P}_2\text{W}_{15}\text{O}_{56}] \cdot 24\text{H}_2\text{O}$ (0.450 g, 0.102 mmol) was dissolved in 9 mL of 0.5 M CH_3COONa buffer (pH 4.2) under vigorous stirring. Solid $\text{Pd}(\text{NO}_3)_2 \cdot 2\text{H}_2\text{O}$ (0.075 g, 0.281 mmol) was added to the obtained solution and the reaction mixture was stirred for another 60 min at room temperature and then filtered and left for evaporation at room temperature being divided into 2–3 vials. Brown crystals of **Na-1** (rhombic plates) form within 1–2 weeks. The crystals were collected by filtration, washed with ice-cold water and dried in air. Yield: 0.27 g (55% based on $\{\text{P}_2\text{W}_{15}\}$). Elemental analysis: calculated for $\text{H}_{142}\text{Na}_{16}\text{O}_{183}\text{P}_4\text{Pd}_4\text{W}_{30}$ (found): Na, 3.87 (3.86); P, 1.30 (1.32); Pd, 4.48 (4.48); W, 58.03 (58.0)%. IR spectrum (KBr pellet), cm^{-1} : 3434 (s, br); 1621 (s); 1090 (s); 1065 (m); 1016 (m); 941 (s); 909 (s); 831 (s); 767 (s); 598 (m); 563 (m); 527 (m); 394 (w); 376 (w). Raman (in solid), cm^{-1} : 984 (s); 964 (s); 887 (m); 822 (w); 526 (w); 374 (w); 324 (w); 226 (w); 164 (w); 118 (w). ^{31}P NMR ($\text{H}_2\text{O}/\text{D}_2\text{O}$): *anti-1*, δ : –3.4, –14.6 ppm; *syn-1*, δ : –3.6, –14.6 ppm. ^{183}W NMR ($\text{H}_2\text{O}/\text{D}_2\text{O}$): *anti-1*, δ : –87 (2 W), –136 (2 W), –155 (2 W), –158 (1 W), –159.5 (2 W), –236 (2 W), –243 (2 W), –245.4 (2 W) ppm; *syn-1*, δ : –91 (2 W), –136 (2 W), –156 (2 W), –

159 (1 W), -160.4 (2 W), -236.6 (2 W), -243.6 (2 W), and -244.6 (2 W) ppm. UV-Vis (0.5 M CH₃COONa buffer solution, pH 4.3): $\lambda = 236$ nm, $\epsilon = 166167$ M⁻¹cm⁻¹; $\lambda = 292$ nm, $\epsilon = 81495$ M⁻¹cm⁻¹; $\lambda = 477$ nm, $\epsilon = 2374$ M⁻¹cm⁻¹.

Synthesis of [(C₄H₉)₄N]₁₅[HPd₄(α -P₂W₁₅O₅₆)₂] (TBA-1). A solution of **Na-1** (0.100 g, 0.010 mmol) in 3 mL of H₂O was dropwise added to an aqueous solution of [(C₄H₉)₄N]HSO₄ (0.080 g, 0.236 mmol, 2 mL of H₂O) under vigorous stirring. The mixture was acidified with 1 drop of 2M HNO₃. The obtained precipitate of **TBA-1** was filtered on a glass frit, washed with plenty of water, and dried in air. Elemental analysis: calculated for C₂₄₀H₅₄₁N₁₅O₁₁₂P₄Pd₄W₃₀ (found): C, 25.08 (24.04); H, 4.74 (4.77); N, 1.83 (1.90)%. IR spectrum (KBr pellet), cm⁻¹: 3468 (m, br); 2961 (s); 2934 (m); 2873 (m); 1630 (w); 1484 (m); 1383 (m); 1237 (w); 1167 (m); 1094 (s); 1064 (m); 1025 (w); 999 (w); 958 (s); 902 (s); 779 (s, br); 597 (m); 595 (m); 560 (m); 530 (m); 430 (w); 392 (m).

X-ray Crystallography. Single-crystal diffraction data for **Na-1** were collected on a SuperNova (Agilent Technologies) diffractometer with MoK α radiation ($\lambda = 0.71073$ Å) at 120 K. A crystal was mounted in a Hampton cryoloop with Paratone-N oil to prevent water loss. Absorption corrections were applied numerically based on multifaceted crystal model using CrysAlis software.¹⁸ The SHELXTL software package¹⁹ was used to solve and refine the structure. The structure was solved by direct methods and refined by full-matrix least-squares method against $|F|^2$ with anisotropic thermal parameters for all heavy POM skeleton atoms (Pd, P, W) and sodium counteranions. The hydrogen atoms of the crystal waters were not located. The relative site occupancy factors for the disordered positions of tungsten, palladium and oxygen atoms due to the {Pd₄P₂W₁₅} / {P₂W₁₅} ligands rotation by 60° were refined using the PART instruction combined with EADP restrictions for the heavy atoms and then fixed at the

obtained values and refined normally. The relative site occupancy factors for the disordered solvent oxygens were first refined in an isotropic approximation with $U_{\text{iso}} = 0.05$ and then fixed at the obtained values and refined without the thermal parameters restrictions.

The number of crystal water molecules and sodium countercations found by XRD was smaller than that determined by elemental analysis (32 vs 71 for H₂O and 7 vs 16 for Na⁺, respectively) which could be explained by the high degree of disorder in the solid-state structure of **Na-1**. This is also consistent with large solvent-accessible volume remained in the structure. For the overall consistency the formula shown in the CIF file corresponds to the bulk material and has the same number of countercations and crystallization water molecules as found by elemental analysis since all the further studies are / will be performed on the isolated bulk material of **Na-1**.

Additional crystallographic data are summarized in Table 1. Further details on the crystal structure investigation may be obtained from Fachinformationszentrum Karlsruhe, 76344 Eggenstein-Leopoldshafen, Germany [fax (+49) 7247-808-666; e-mail crysdata@fiz-karlsruhe.de), upon quoting the depository number CSD 428389.

Table 1. Crystal data and structure refinement for **Na-1**

Empirical formula	H ₁₄₂ Na ₁₆ O ₁₈₃ P ₄ Pd ₄ W ₃₀
Formula weight, g/mol	9503.96
Crystal system	Triclinic
Space group	<i>P</i> -1
<i>a</i> , Å	14.0333(3)
<i>b</i> , Å	14.0985(3)
<i>c</i> , Å	25.2703(5)
α	83.9425(17)°

β	76.5160(19)°
γ	60.514(2)°
Volume, Å ³	4231.88(16)
Z	1
D_{calc} , g/cm ³	3.729
Absorption coefficient, mm ⁻¹	20.912
$F(000)$	4246
Crystal size, mm	0.06 × 0.06 × 0.13
Theta range for data collection	4.09° – 25.03°
Completeness to θ_{max}	98.5%
Index ranges	$-16 \leq h \leq 16$, $-16 \leq k \leq 16$, $-30 \leq l \leq 30$
Reflections collected	75309
Independent reflections	14717
R_{int}	0.0722
Observed ($I > 2\sigma(I)$)	13246
Absorption correction	Empirical using spherical harmonics
$T_{\text{min}} / T_{\text{max}}$	0.0822 / 0.3732
Data / restraints / parameters	14717 / 24 / 663
Goodness-of-fit on F^2	1.109
R_1 , wR_2 ($I > 2\sigma(I)$)	$R_1 = 0.0722$, $wR_2 = 0.1829$
R_1 , wR_2 (all data)	$R_1 = 0.0781$, $wR_2 = 0.1874$
Largest diff. peak and hole, e. Å ⁻³	3.876 and -3.061

ACKNOWLEDGMENT

Financial support was provided to P.K. by the European Commission (ERC Starting Grant MOLSPINTRON, no. 308051).

ASSOCIATED CONTENT

Supporting Information. Crystallographic data in CIF format, IR spectra and UV-Vis spectra; structure of $\{P_2W_{15}\}$ and its vacant site and comparison of the $\{Pd_4(P_2W_{15})_2\}$ structure with the structures of $\{M_4(P_2W_{15})_2\}$ and $\{Pd_3(XW_9)_2\}$ polyanions. This material is available free of charge via the Internet at <http://pubs.acs.org>.

AUTHOR INFORMATION

Corresponding Author

*E-mail: paul.koegerler@ac.rwth-aachen.de

Author Contributions

The manuscript was written through contributions of all authors. All authors have given approval to the final version of the manuscript.

ABBREVIATIONS

POT: polyoxotungstate; POM: polyoxometalate.

REFERENCES

- (1) (a) Neumann, R.; Khenkin, A. M. *Inorg. Chem.* **1995**, *34*, 5753-5760; (b) Kuznetsova, N. I.; Detusheva, L. G.; Kuznetsova, L. I.; Fedotov, M. A.; Likholobov, V. A. *J. Mol. Catal. A: Chem.* **1996**, *114*, 131-139; (c) Gazarov, R. A.; Shirokov, V. A.; Petrov, P. A.; Dyatlov, V. A.;

Egorov, Yu. A. Patent of Russian Federation No. 2064828, **1996**; (d) Neumann, R.; Khenkin, A. M.; Juwiler, D.; Miller, H.; Gara, M. *J. Mol. Catal. A Chem.* **1997**, *117*, 169-183; (e) Vorontsova, I. V.; Korovchenko, P. A.; Gazarov, R. A. *Mendeleev Chem. J.* **1998**, *42*, 242-247; (f) Xie, Y.; Sun, W. L.; Liu, H. Z.; Kong, J. L.; Xie, G. Y.; Deng, J. Q. *Chem. Res. Chin. Univ.* **1998**, *14*, 87-89; (g) Xie, Y.; Sun, W. L.; Liu, H. Z.; Kong, J. L.; Xie, G. Y.; Deng, J. Q. *Analytical Lett.* **1998**, *31*, 2009-2024; (h) Duan, D.-L.; Wang, Z.-Z.; Gu, Y.-W.; Yang, A.-M. *Yunnan Daxue Xuebao, Ziran Kexueban* **2001**, *23*, 447-453; (i) Kogan, V.; Aizenshtat, Z.; Neumann, R. *New J. Chem.* **2002**, *26*, 272-274; (j) Adam, W.; Alsters, P. L.; Neumann, R.; Saha-Möller, C. R.; Sloboda-Rozner, S.; Zhang, R. *J. Org. Chem.* **2003**, *68*, 1721-1728; (k) Adam, W.; Alsters, P. L.; Neumann, R.; Saha-Möller, C. R.; Seebach, D.; Beck, A.; Zhang, R. *J. Org. Chem.* **2003**, *68*, 8222-8231; (l) Stapleton, A. J.; Sloan, M. E.; Napper, N. J.; Burns, R. C. *Dalton Trans.* **2009**, 9603-9615; (m) Hirano, T.; Uehara, K.; Kamata, K.; Mizuno, N. *J. Am. Chem. Soc.* **2012**, *134*, 6425-6433; (n) Tong, J. H.; Wang, H. Y.; Cai, X. D.; Zhang, Q. P.; Ma, H. C.; Lei, Z. Q. *Appl. Organomet. Chem.* **2014**, *28*, 95-100; (o) Villanneau, R.; Roucoux, A.; Beaunier, P.; Brourief, D.; Proust, A. *RSC Adv.* **2014**, *4*, 26491-26498.

(2) (a) Putaj, P.; Lefebvre, F. *Coord. Chem. Rev.* **2011**, *255*, 1642-1685; (b) Izarova, N. V.; Pope, M. T.; Kortz, U. *Angew. Chem. Int. Ed.* **2012**, *51*, 9492-9510.

(3) (a) Chubarova, E. V.; Dickman, M. H.; Keita, B.; Nadjö, L.; Miserque, F.; Mifsud, M.; Arends, I. W. C. E.; Kortz, U. *Angew. Chem. Int. Ed.* **2008**, *47*, 9542. (b) Izarova, N. V.; Vankova, N.; Heine, T.; Ngo Biboum, R.; Keita, B.; Nadjö, L. Kortz, U. *Angew. Chem. Int. Ed.* **2010**, *49*, 1886-1889; (c) Izarova, N. V.; Kondinski, A.; Vankova, N.; Heine, T.; Jäger, P.; Schinle, F.; Hampe, O.; Kortz, U. *Chem. Eur. J.* **2014**, *20*, 8556-8560.

- (4) Cameron, J. M.; Gao, J.; Long, D.-L.; Cronin, L. *Inorg. Chem. Front.* **2014**, *1*, 178-185.
- (5) (a) Angus-Dunne, S. J.; Burns, R. C.; Craig, D. C.; Lawrance, G. A. *J. Chem. Soc., Chem. Commun.* **1994**, 523-524; (b) Maksimov, G. M.; Maksimovskaya, R. I.; Matveev, K. I. *Rus. J. Inorg. Chem.* **1987**, *32*, 551-555; (c) Izarova, N. V.; Banerjee, A.; Kortz, U. *Inorg. Chem.* **2011**, *50*, 10379-10386.
- (6) Hirano, T.; Uehara, K.; Uchida, S.; Hibino, M.; Kamata, K.; Mizuno, N. *Inorg. Chem.* **2013**, *52*, 2662-2670.
- (7) (a) Knoth, W. H.; Domaille, P. J.; Harlow, R. L. *Inorg. Chem.* **1986**, *25*, 1577-1584; (b) Detusheva, L. G.; Kuznetsova, L. I.; Fedotov, M. A.; Likholobov, V. A.; Dovlitova, L. S.; Vlasov, A. A.; Malakhov, V. V. *Russ. J. Coord. Chem.* **2001**, *27*, 838-845; (c) Villanneau, R.; Renaudineau, S.; Herson, P.; Boubekur, K.; Thouvenot, R.; Proust, A. *Eur. J. Inorg. Chem.* **2009**, 479-488; (d) Bi, L.-H.; Kortz, U.; Keita, B.; Nadjó, L.; Borrmann, H. *Inorg. Chem.* **2004**, *43*, 8367-8372.
- (8) (a) Krebs, B.; Droste, E.; Piepenbrink M. in *Polyoxometalate Chemistry. From Topology via Self-Assembly to Applications*; Pope, M. T., Müller, A. Eds.; Kluwer, Dordrecht, **2001**, pp. 89 – 99; (b) Bi, L.-H.; Reicke, M.; Kortz, U.; Keita, B.; Nadjó, L.; Clark, R. J. *Inorg. Chem.* **2004**, *43*, 3915-3920; (c) Bi, L.-H.; Kortz, U.; Keita, B.; Nadjó, L.; Daniels, L. *Eur. J. Inorg. Chem.* **2005**, 3034-3041; (d) J. Gao, J. Yan, S. Beeg, D.-L. Long, L. Cronin, *Angew. Chem. Int. Ed.* **2012**, *51*, 3373-3376.
- (9) Bi, L.-H.; Dickman, M. H.; Kortz, U. *CrystEngComm* **2009**, *11*, 965-966

(10) Sokolov, M. N.; Kalinina, I. V.; Peresypkina, E. V.; Moroz, N. K.; Naumov, D. Y.; Fedin, V. P. *Eur. J. Inorg. Chem.* **2013**, 1772-1779.

(11) See for example: (a) Finke, R. G.; Droege, M. W. *Inorg. Chem.* **1983**, 22, 1006–1008; (b) Finke, R. G.; Droege, M. W.; Domaille, P. J. *Inorg. Chem.* **1987**, 26, 3886-3896; (c) Weakley, T. J. R.; Finke, R. G. *Inorg. Chem.* **1990**, 29, 1235–1241; (d) Finke, R. G.; Weakley, T. J. R. *J. Chem. Crystallogr.* **1994**, 24, 123-128; (e) Gómez-García, C. J.; Borrás-Almenar, J. J.; Coronado, E.; Ouahab, L. *Inorg. Chem.* **1994**, 33, 4016-4022; (f) Kirby, J. F.; Baker, L. C. W. *J. Am. Chem. Soc.* **1995**, 117, 10010-10016; (g) Zhang, X.; Chen, Q.; Duncan, D. C.; Campana, C.; Hill, C. L. *Inorg. Chem.* **1997**, 36, 4208–4215; (h) Anderson, T. M.; Zhang, X.; Hardcastle, K. I.; Hill, C. L. *Inorg. Chem.* **2002**, 41, 2477–2488; (i) Ruhlmann, L.; Nadjó, L.; Canny, J.; Thouvenot, R. *Eur. J. Inorg. Chem.* **2002**, 975–986; (j) Mbomekalle, I. M.; Keita, B.; Nadjó, L.; Berthet, P.; Hardcastle, K. I.; Hill, C. L.; Anderson, T. M. *Inorg. Chem.*, **2003**, 42, 1163–1169; (k) Mbomekalle, I. M.; Keita, B.; Nadjó, L.; Berthet, P.; Neiwert, W. A.; Hill, C. L.; Ritorto, M. D.; Anderson, T. M. *Dalton Trans.* **2003**, 2646–2650; (l) Ruhlmann, L.; Schaming, D.; Ahmed, I.; Courville, A.; Canny, J.; Thouvenot, R. *Inorg. Chem.* **2012**, 51, 8202–8211; (m) Yao, S.; Yan, J.; Yu, Y.; Wang, E.-B. *J. Coord. Chem.* **2012**, 65, 1451–1458.

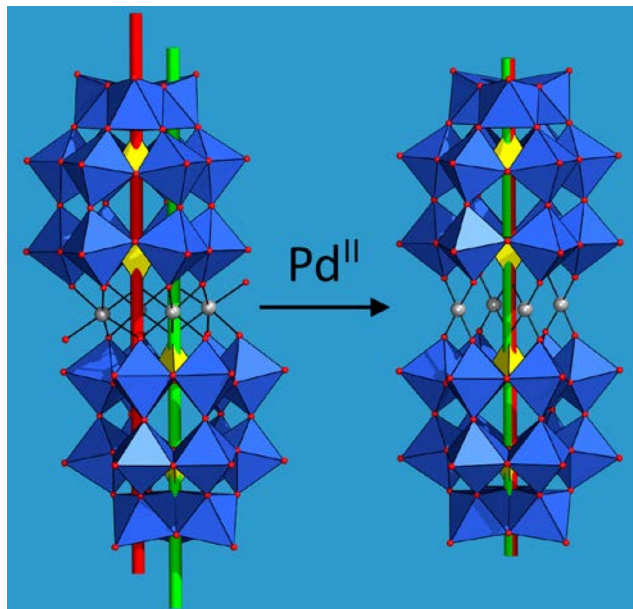
(12) Contant, R. *Inorg. Synth.* **1990**, 27, 104–111.

(13) Wu, H. *J. Biol. Chem.* **1920**, 43, 189-220.

(14) (a) Parker, S. F.; Refson, K.; Hannon, A. C.; Barney, E. R.; Robertson, S. J.; Albers, P. J. *Phys. Chem. C* **2010**, 114, 14164–14172; (b) Barsukova, M.; Izarova, N. V.; Ngo Biboum, R.; Keita, B.; Nadjó, L.; Ramachandran, V.; Dalal, N. S.; Antonova, N. S.; Carbó, J. J.; Poblet, J. M.; Kortz, U. *Chem. Eur. J.* **2010**, 16, 9076–9085.

- (15) Edlund, D. J.; Saxton, R. J.; Lyon, D. K.; Finke, R. G. *Organometallics* **1988**, 7, 1692-1704.
- (16) Kato, C. N.; Kashiwagi, T.; Unno, W.; Nakagawa, M.; Uno, H. *Inorg. Chem.*, **2014**, 53, 4824–4832.
- (17) Meng, L.; Liu, J. F. *Transition Met. Chem.* **1995**, 20, 188-190.
- (18) CrysAlisPro, Agilent Technologies, Version 1.171.36.21 (release 14-08-2012 CrysAlis171.NET).
- (19) Sheldrick G. M. *Acta Cryst.* **2008**, A64, 112-122.

For Table of Contents Only



Pd^{II} -based sandwich complexes of lacunary $\{\text{P}_2\text{W}_{15}\}$ -type polyoxotungstates differ markedly from classical dimeric $\{\text{M}_4(\text{P}_2\text{W}_{15})_2\}$ structures incorporating octahedral first-row transition metal M^{II} centers, form *syn* and *anti* isomers in a characteristic 2:1 ratio and exhibit high stability in solution.